SSM/I Time Series Observations of Great Lakes Ice and Snow

D. PLIANT[1]

ABSTRACT

Special Sensor Microwave Imager (SSM/I) time series data are presented to qualitatively examine regional scale snow and ice phenomena for the Great Lakes winter of 1993-94. Microwave brightness temperature, air temperature and snow accumulation time series for the Keweenaw region of Lake Superior are coplotted for comparison. Image time series are presented showing the winter evolution of Great Lakes ice cover. Same-day SSM/I and Advanced Very High Resolution Radiometer (AVHRR) images of Lake Superior are compared, showing the potential of SSM/I as a regional-scale ice-detection tool.

Key words: ice, snow, Great Lakes, passive microwave, remote sensing.

INTRODUCTION

The Great Lakes hydrologic system is integral to midcontinent weather and climate. Lake ice and snow are important to climate change studies and to the daily lives of the approximately 42,000,000 people living in the Great Lakes-St. Lawrence basin (Center for the Great Lakes, 1995). Lake ice modulates heat and longwave radiation fluxes between lake and atmosphere, controls penetration of shortwave radiation used in photosynthesis, affects shoreline processes and determines the shipping season. Snow modulates shortwave/longwave radiation and heat fluxes between land/ice and atmosphere, as well as being a dominant factor in ground and surface water recharge.

Remote sensing in the microwave portion of the spectrum has been useful in providing information about snow and ice and has led to a number of application in hydrology and climatology (Barry, et al., 1993; Grody, 1991; Foster, et al., 1984). Microwaves are relatively unaffected by atmospheric conditions, permitting imagery to be acquired day or night in all seasons. This is a distinct advantage over visible and infrared imagery, which is daylight and weather sensitive. The principal disadvantage of microwaves is the coarse spatial resolution. The intensity of earth microwave emission is relatively low, requiring larger field of views to obtain an adequate signal to noise ratio.

This paper presents primarily qualitative observations of Great Lakes ice and snow for the winter of 1993-94 (the time period was selected based on data availability, and the author's related but unreported field work). One objective is to gain basic insight regarding the passive microwave expression of the Great Lakes water and landscape changing through a winter season.

The passive microwave data are described, and the problem of missing pixels addressed through averaging. Graphs of air temperature, snow accumulation and microwave brightness temperature are used to display interrelationships among these variables. Time series of microwave imagery display the geophysical evolution of the landscape through the winter at the 10-1000 km scale. The paper concludes with comments on ice detectability using SSM/I as verified by AVHRR thermal infrared data.

DATA AND PROCESSING

The Special Sensor Microwave Imager is a meteorological instrument aboard the Department of Defense DMSP satellites (Hollinger, et al. 1987; DMSP, 1995). There are four frequencies (GHz) and two polarizations (seven channels in total): 19h, 19v, 22v, 37h, 37v, 85h, 85v (h/v = horizontal/vertical polarization). The sensor measures the intensity of upwelling radiation emitted by land, water and atmosphere in the instrument field of view, typically reported in units of brightness temperature (T_B, in degrees Kelvin). Brightness temperature is defined as (Fung and Ulaby, 1983, eq. 4-45):

$$T_B = e^*T$$

where e=object emissivity and T=object physical temperature.

The SSM/I data used here are from the DMSP F-11 Brightness Temperature Grids (CD-ROM) series produced by the National Snow and Ice Data Center

[1] Department of Geological Engineering and Sciences, Michigan Technological University, Houghton, Michigan 49931, Internet: anpilant@mtu.edu, URL: http://www.geo.mtu.edu

(NSIDC, 1995). Raw data on CD are brightness temperatures on a polar stereographic projection binned to 12.5 km (85 GHz) and 25 km (19, 22 and 37 GHz) pixels with a 0.1° K radiometric resolution. The daily ascending and descending satellite passes are averaged at NSIDC, thereby assigning a single daily T_B value to each grid position for each channel. The entire winter of 1993-94 is available on one CD, in all seven frequency-polarization combinations. Horizontal polarization (H pol.) is used in this analysis because of the stronger contrast between water and non-water.

There are pervasive data dropouts at this latitude due to tape recorder failures onboard the F11 satellite, leading to degradation of this data set (Figure 1). To generate a more consistent image time series, each pixel on each date was averaged over the three preceding and subsequent dates, thus filling in missing pixels. Averaging reduces the radiometric fidelity of the T_B data, but provides a much cleaner data set for visual interpretation. Visual inspection of numerous images indicates that a seven-day average provides a relatively complete image (i.e., few missing pixels) for a given day in the time series. Comparison of raw and averaged data (Figure 2) shows RMS errors of ~ 3% for land T_B and ~ 11% for lake T_B (37 GHz); the correlation is adequate for this qualitative study of regional-scale phenomena. The larger RMS error of averaged lake T_B is probably due to more rapidly changing conditions on the lake (due to drifting ice and changes in water surface roughness).

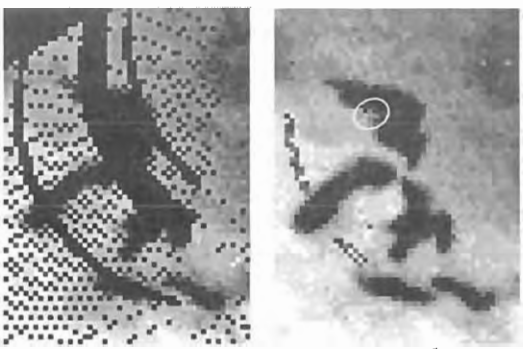

Figure 1. Comparison of a raw and averaged SSM/I images for the Great Lakes (3 January 1994, 37 GHz H pol.). Black pixels and swaths are missing data. All channels and most dates are similarly degraded. White ellipse indicates region of land/water T_B samples plotted in Figure 3.

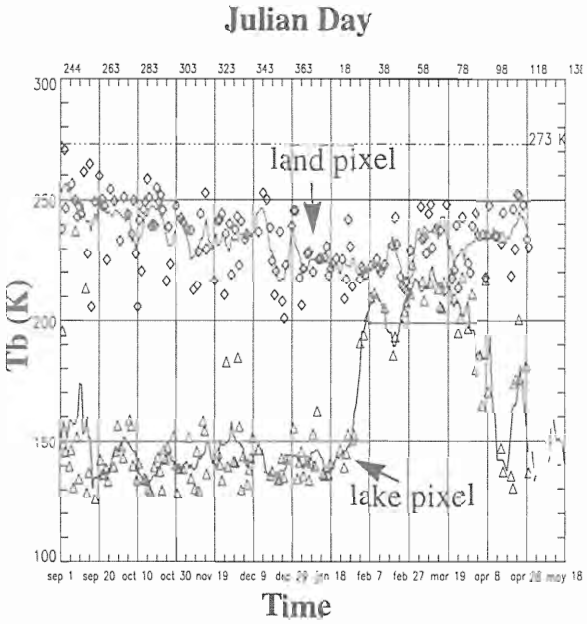

Figure 2. Comparison of raw and averaged T_B (37 GHz H pol.) for one land and one lake pixel through the 1993-94 winter. Lines = averaged T_B Diamonds = raw land T_B. Triangles = raw lake T_B. RMS error land = 9.9 K. RMS error lake = 14.7 K. Missing pixels were omitted from computation. The 70° K "hump" in the lake pixel graph indicates the presence of ice, with higher emissivity, at the pixel location.

DISCUSSION

Interrelationships among time series of air temperature, snow accumulation and brightness temperature are apparent in Figure 3. Graphs of daily air temperature and snow depth/daily accumulation are from the Michigan Technological University (MTU) on-campus weather station. Brightness temperature (85 GHz) histories of three land and three lake pixels are graphed. Each pixel was selected to be relatively proximal to the MTU weather station but far enough (>12.5 km) from the narrow peninsula to be either completely land or completely water (i.e., not mixed pixels).Interpretations of Figure 3 build upon visual inspection of computer animations of microwave image time series which could not be included here. *(Computer animated image time series sequences are available online on the World Wide Web at the following URL: http://www.geo.mtu.edu).*

Figures 4 and 5 are time series of 85 and 37 GHz images spaced at 20 day intervals (corresponding to the vertical grid lines in Figure 3). The relatively high spatial resolution (12.5 km) of the 85 GHz data

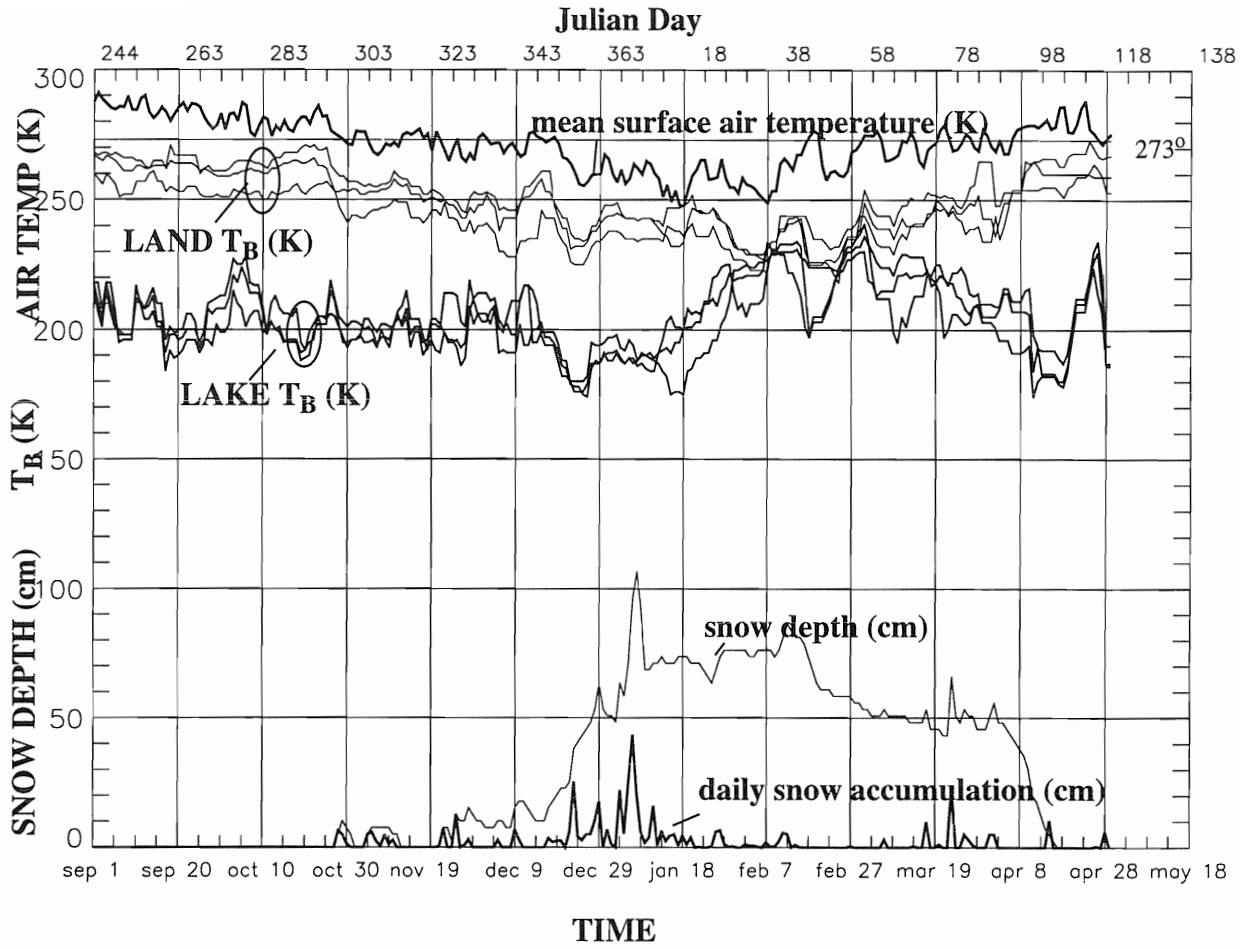

Figure 3. Time series of air temperature, brightness temperature and snow accumulation near MTU in northern Michigan. Horizontal axis = time in days. The vertical axis scales daily mean surface air temperature (K), snow depth/daily accumulation (cm) and brightness temperature (K) (85 GHz, H-pol). The land Tb graph is a time series for a single averaged land pixel. Three land and three lake pixels are plotted (approximate pixel locations are indicated in Figure 1).

enhances interpretability. The 37 GHz data (25 km pixels) are included because this frequency is commonly used in cryospheric studies, 37 GHz being the frequency most sensitive to snow grain size.

Land T_B

Land T_B (Figure 3) parallels air temperature relatively closely as might be expected, despite averaging. It decreases in a subtle manner with air temperature as winter progresses, dropping only ~5-10 K while air temperature drops 30 K between September 1 and February 7. Local T_B minima and maxima follow air temperatures, reflecting the linear dependence of T_B on physical temperature.

Lake T_B

Lake T_B (Figure 3) shows a fascinating history of ice development and decay. The open water period spans ~September 1-January 10. Lake T_B is low, in the range of ~190-210 K. Lake T_B drops ~5-10 K with air temperature, but does not parallel local air temperature minima and maxima to the degree that land T_B does.

Ice begins forming in early January, indicated by the increase in lake T_B from ~180-200 K to 230-250 K. Ice emissivity is higher than that of water at 85 GHz, so it appears radiometrically brighter. The "hump" spanning ~January 13-April 3 corresponds approximately to the period of ice development and decay visible for the entire lake in the complete image time series (computer animations). The sharp drop on February 17 is probably a mixed water-ice signal resulting from wind drifting north and east of the Keweenaw Peninsula. Ice returned in subsequent days, producing a corresponding increase in T_B.

The decrease in lake T_B spanning ~February 27-

April 8 resulted from decreasing ice concentration (increasing open water fraction) in the pixels as breakup proceeded. The two small humps between ~April 8 and 28 are probably ephemeral periods of increased drift ice concentration.

Snow accumulation

The daily snow accumulation graph is characteristic of the lake effect snow history in this region. The onset of snow accumulation coincides with the mean daily air temperature decreasing below 0° C. Daily snow accumulation is inversely related to lake T_B. As ice cover increases (indicated by increasing lake T_B), open water available for evaporation decreases, limiting water vapor available for lake effect snow. Daily snow accumulation decreases to a few cm/day around January 13, coinciding with the increase in lake T_B marking the onset of local ice development. There are only a few sporadic snow events between January 28 and March 17, coinciding with the period of maximum areal extent of ice cover. Three 5-20 cm snow events occur in late March as lake T_B returns to its background water value (circa April 3, ~200 K), signalling a movement toward dominantly unfrozen conditions. Snow accumulation effectively ceases near the peak in the lake T_B graph around February 1, coinciding with the period of maximum areal extent of lake ice as indicated by the image time series.

85 and 37 GHz image time series

The 85 and 37 GHz image time series (Figures 4 and 5) are similar in overall character. The following remarks apply to both image sequences.

Pre-snow conditions in October are indicated by radiometrically warm land and cold water. By November 19, snow has begun to accumulate in the northern regions, lowering land T_B (darkening the image). Ice begins forming in western and eastern Lake Superior by January 18 (brightening the image). Lakes Superior, Huron and Erie are extensively ice covered on February 7 and 27. Land T_B is darkest in this interval, suggesting lowest temperatures and maximum snow pack thickness (see also Figure 3). March 19 and April 8 images show the effect of northwest winds concentrating ice in southeast portions of Lakes Superior, Huron and Erie during ice breakup. Lakes Michigan and Ontario maintain lesser ice coverage.

Comparison of AVHRR and SSM/I images

Figure 6 is a thermal infrared AVHRR image acquired at approximately 10 a.m. local time on March 12, and an 85 GHz SSM/I image from the same date (the average of the day's ascending and descending passes). Two principal points emerge. The spatial resolution of the AVHRR image (1.1 km) is superior to SSM/I (12.5 km) for ice identification/concentration studies. However, note the general agreement in patterns of image tone, indicating that the SSM/I image can roughly delimit presence and absence of ice in a given region of the lake, and provide an estimate of total ice cover over the lake. Two or more SSM/I images are available each day. AVHRR data are acquired twice daily, but clouds obscure the lake more than not. The NOAA Satellite Active Archive (SAA, 1995) was searched for a set of AVHRR images for March 1994. Only five images were obtained that contained less then ~30% cloud cover over Lake Superior. This highlights the ice-detection utility of an all weather, day-night microwave sensor such as SSM/I or a radar (e.g., ERS-1/2, RADARSAT).

CONCLUSIONS

This paper attempts to illuminate some of the broad-scale interrelationships among microwave brightness temperature, air physical temperature and snow accumulation for the Keweenaw region of Lake Superior. The timing of Lake Superior ice development and decay is tracked by following T_B time series for land and lake pixels. The suppression of lake effect snow by ice cover growth is demonstrated. The seasonal changes of land and lake brightness temperature are displayed in time series of 85 and 37 GHz imagery. SSM/I data have the potential to enhance Great Lake ice monitoring programs, especially if used in concert with AVHRR data. Ultimately, synthetic aperture radar data may provide superior spatial and textural information, but with an associated increase in data costs.

The NSIDC SSM/I brightness temperature grids on CD-ROM provide straightforward access to passive microwave data for Great Lakes snow and ice studies. These data are well suited to spatially and temporally synoptic time series analysis, and to observing lake ice cover timing, duration, presence/absence and possibly concentration. Limitations of this particular data product are missing pixels (at this latitude) and a single daily T_B value. Other NSIDC data products are increasingly available that provide separate ascending and descending pass T_B values. Missing pixels were accommodated in this study by averaging, with a consequent decrease in radiometric resolution to within approximately 3% (land) and

11% (lake) of the original T_B. A single daily T_B value is limiting in studies requiring high radiometric and temporal resolution, or in spring time when freeze-thaw cycles in the snowpack yield large T_B differences depending upon melt conditions. Computer animation of microwave image time series was found to provide a powerful tool for visualization of time-dependent regional-scale snow and ice conditions.

ACKNOWLEDGEMENTS

The author thanks Jim Carstens for MTU weather station data, NSIDC for SSM/I data, Bob Landsparger, Matt Wacholz and John Gierke for computer support and Bono Sen, Gregg Bluth, David Delene and anonymous reviewers for helpful comments. This research is funded by NASA Graduate Student Fellowship for Global Change Research #1956-GC920312.

REFERENCES

Barry, R.G., Armstrong, R.L., and Krenke, A.N., 1993. An approach to assessing changes in snow cover- an example from the former Soviet Union: in 50th Anniversary Proc. Eastern Snow Conference, June 8-10, 1993, Quebec City, Quebec, p. 25-33.

DMSP, 1995. URL- http://web.ngdc.noaa.gov/dmsp/ssmi.html

Foster, J.L, Hall, D.K., and Chang, A.T.C., 1984. An overview of passive microwave snow research and results: Reviews of Geophysics and Space Physics, v. 22, no. 2, p. 195-208.

Fung, A.K. and Ulaby, F.T., 1983. Matter-energy interaction in the microwave region, in Manual of Remote Sensing, Second Ed., Am. Soc. Photogrammetry, Vol. 1, p. 115-164.

Grody, N.C., 1991. Classification of Snow Cover and Precipitation Using the Special Sensor Microwave Imager: Jour. Geophysical Research, v. 96, no. D4, pp. 7423-7435.

Hollinger, J., Lo, R, Poe, G., Savage, R. and Pierce, J., 1987. Special Sensor Microwave/Imager User's Guide, Naval Research Laboratory, Washington, DC, 120 pp.

NSIDC, 1995. URL- http://nsidc.colorado.edu/NSIDC/Services.html

SAA, 1995. NOAA Satellite Active Archive: URL-http://www.saa.noaa.gov.

The Center for the Great Lakes, 1995. About Climate Change and the Great Lakes Economy: URL- http://gopher.great-lakes.net:2200/0/waterairland/global-warming/clmth2o.inf.

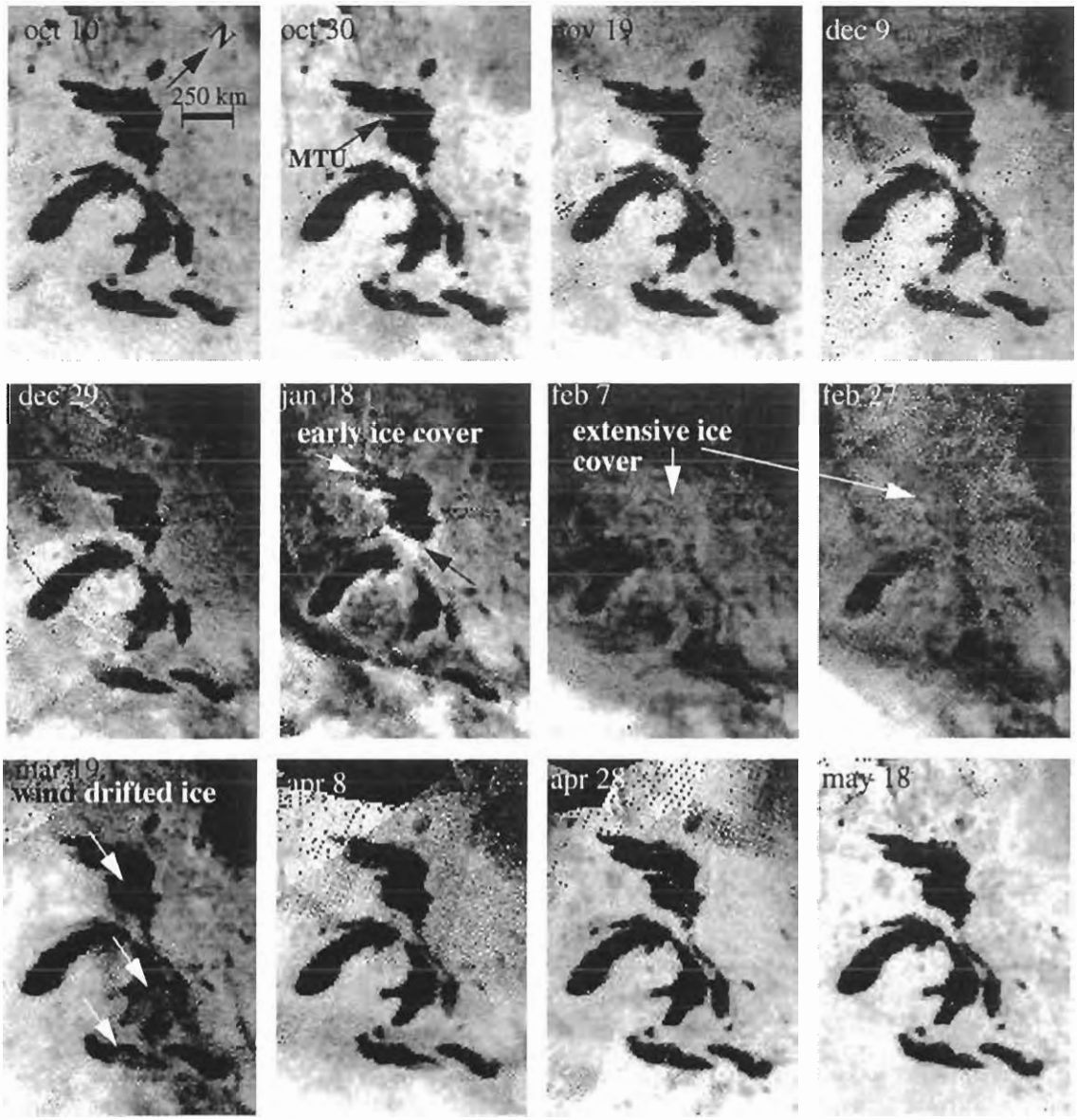

Figure 4. Image time series of 85 GHz H pol. T_B spanning winter 1993-94. Image brightness is proportional to T_B.

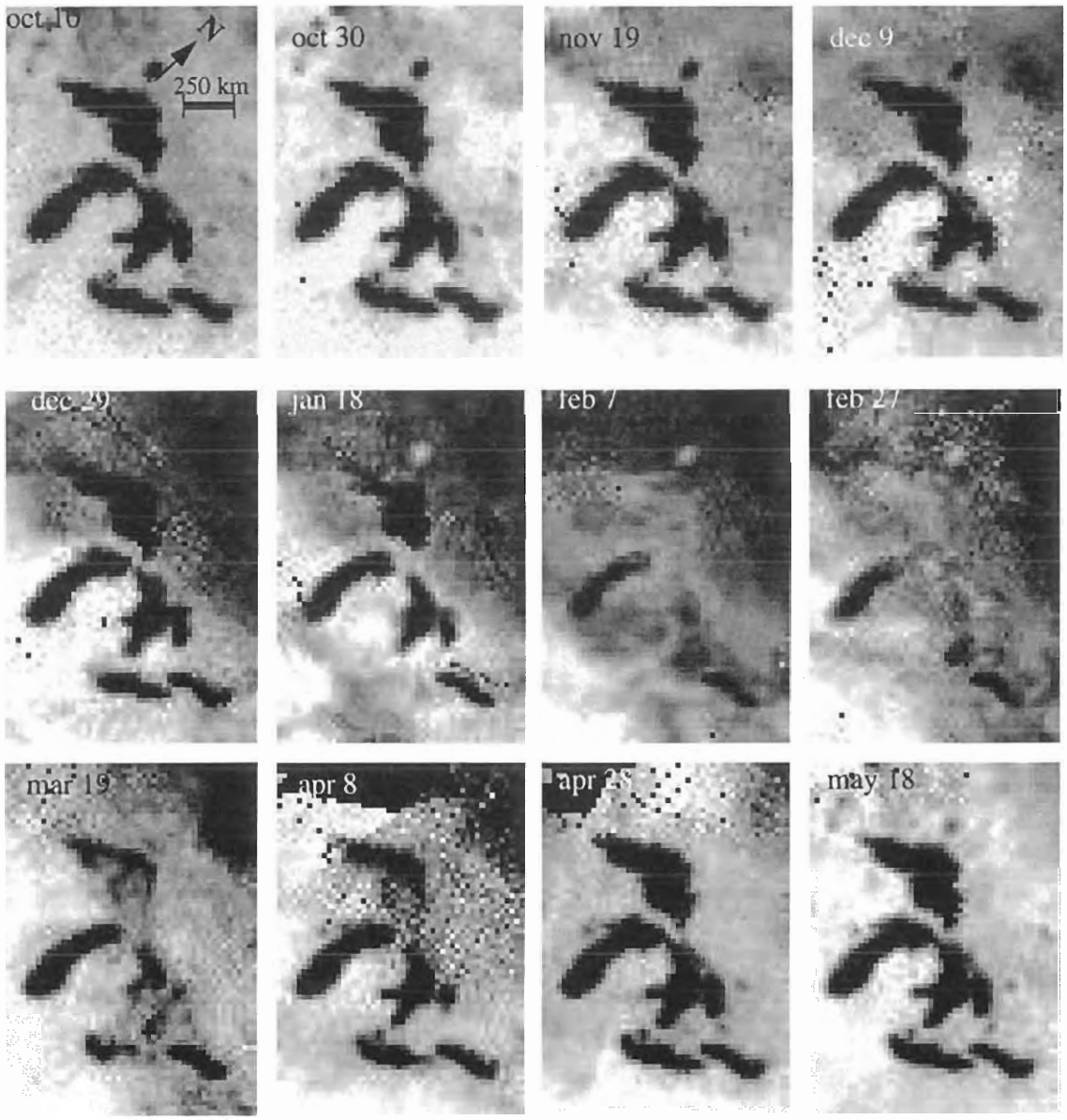

Figure 5. Image time series of 37 GHz H pol. T_B spanning winter 1993-94.

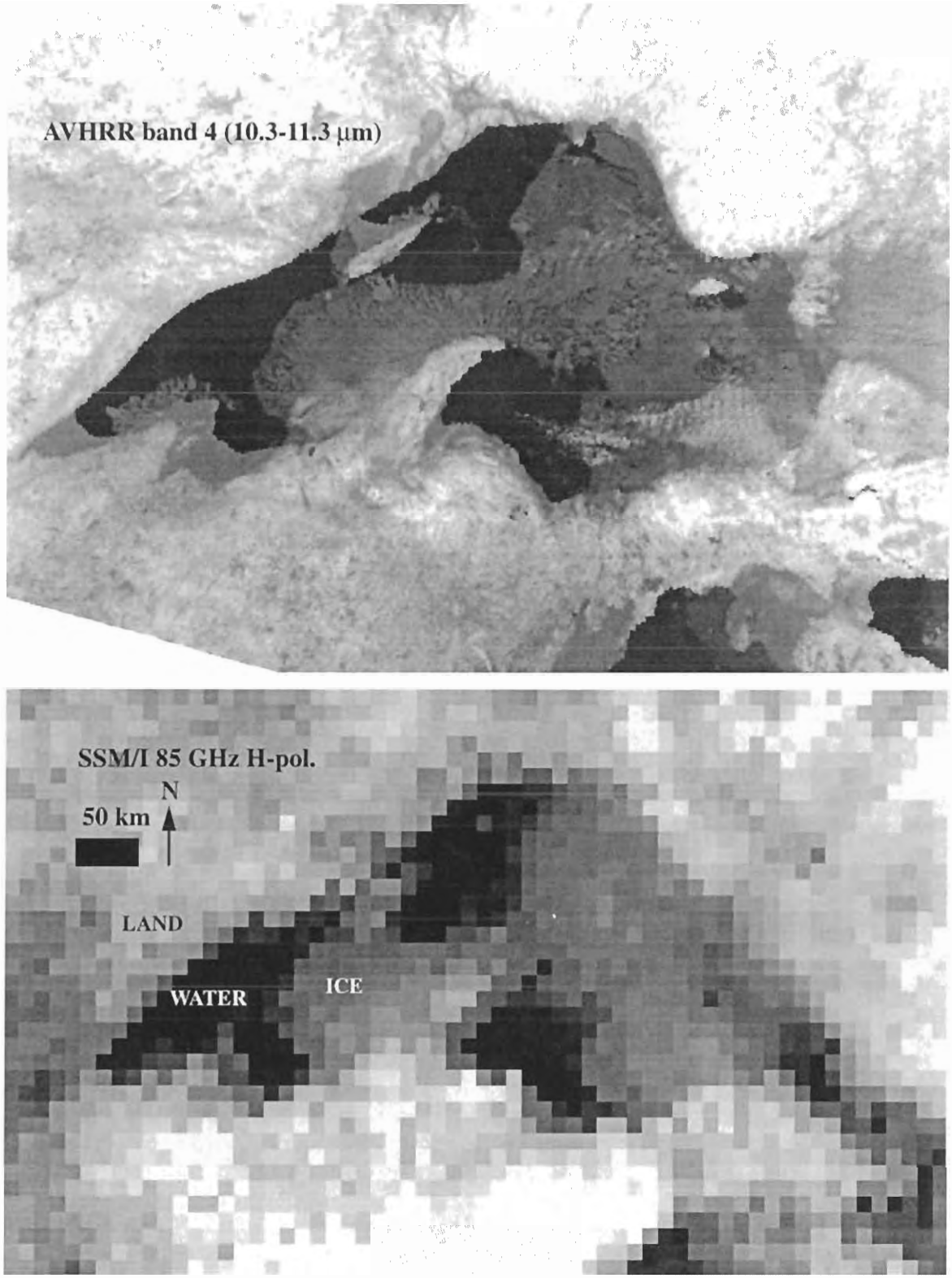

Figure 6. AVHRR and SSM/I images of Lake Superior on 9 March 1994. Water is black, ice is medium grey tones, land is grey-white tones. Note the difference in spatial resolutions (AVHRR: 1.1 km; SSM/I: 12.5 km) and degree of ice detectability using SSM/I.